

# The Milky Way Tomography with SDSS: II. Stellar Metallicity (Appendix C)

Ivezić et al. 2008, submitted to ApJ (sdss-pub 772)

## Appendix C. Photometric Parallax Relation Derived using Globular Clusters

In Paper I, we proposed a photometric parallax relation that did not explicitly use metallicity information, because of two main reasons. First, the analysis included stars close to the faint limit of SDSS imaging for which the accuracy of photometric metallicity is significantly deteriorated due to increased  $u$  band noise, and, second, the sample also included red stars for which metallicity is hard to estimate. The photometric parallax relation adopted in Paper I implicitly takes metallicity effects into account by being somewhat shallower than a photometric parallax relation appropriate for a single-metallicity population: nearby stars ( $\lesssim 1$  kpc, or so), which are predominantly red (due to flux-limited sample,  $r > 14$ ), have on average high disk-like metallicities, while distant stars ( $\sim 1$ -10 kpc) are predominantly blue stars with low metallicities (at a given  $g - r$  or  $g - i$  color, luminosity increases with metallicity for main-sequence stars). However, here we discuss only stars for which photometric metallicity estimates are available and, furthermore, they do not include very faint stars due to the flux limit ( $u \lesssim 21$ ) imposed by requiring proper motion information. Hence, we can explicitly account for shifts of photometric parallax relation as a function of metallicity.

The color-magnitude diagrams for globular clusters can be used to constrain the photometric parallax relation and its dependence on metallicity, and to estimate systematic errors using the residuals between the adopted relation and individual clusters. For example, using three fiducial cluster sequences,  $M_V(B - V)$ , corresponding to metallicities,  $[Fe/H]$ , of  $-2.20$ ,  $-0.71$  and  $+0.12$ , Beers et al. (2000) spline interpolate between them to get  $M_V$  for an arbitrary combination of  $B - V$  and  $[Fe/H]$ . This is the method used to compute main-sequence distance estimates available from SDSS Data Release catalogs.

There are several reasons to revisit the method developed by Beers et al. First, a transformation from Johnson system to SDSS system is required to apply their method to SDSS data. While this transformation is known to about 0.01 mag (Ivezić et al. 2007), even such a small systematic error results in an uncertainty of absolute magnitude of  $\sim 0.12$  mag for blue stars. Second, only three fiducial color-magnitude sequences are utilized and it is not clear whether spline interpolation captures in detail the shift of main sequence as a function of metallicity. Third, the impact of age variations on the assumed absolute magnitudes is not quantitatively known. Furthermore, it is not known how similar are

color-magnitude sequences for different clusters with similar metallicity. It is, therefore, desirable to determine photometric parallax relation using a larger number of clusters, with at least some of them observed by SDSS.

We use five globular clusters observed by SDSS, selected to have distance in the range 7–12 kpc (using distances from Harris 1996), to constrain the *shape* of the photometric parallax relation. This distance range ensures sufficient photometric quality for stars in the color range  $g - i < 0.8$  ( $g - r \lesssim 0.6$ ) where photometric metallicity estimates are reliable. We augment this sample by data for six additional clusters compiled by VandenBerg & Clem (2003), which significantly increase the sampled metallicity range and allow us to determine the shift of photometric parallax relation as a function of metallicity. We use additional clusters observed by SDSS and by Clem, VandenBerg & Stetson (2008), as well as constraints based on Hipparcos and ground-based trigonometric parallax measurements, to test the adopted photometric parallax relation.

### C.1 Methodology and Results

For clusters observed by SDSS, we select candidate cluster stars by limiting their angular distances from the cluster center to be less than the cluster radius determined by Simones, Newberg & Cole (2008). These radii, and distance and metallicity data from Harris (1996), are listed in Table 5. While the faint flux limits of SDSS imaging data limit this analysis only to relatively blue stars ( $g - i < 1.0$ ), the color range where photometric metallicity can be determined is fully covered.

For each cluster, we determine the median  $r$  band magnitude in 0.05 mag wide bins of the  $g - i$  color. The red limit for the considered  $g - i$  range is set by requiring  $r < 21.5$ , and the blue end is selected to be at least 0.05 mag redder than the vertical part of the observed sequences (turn-off stars). The red limit ensures sufficient signal-to-noise ratios, and the blue limit is designed to minimize the evolutionary (age) effects on the shape of adopted relation. That is, we deliberately construct a relation that corresponds to small ages first, and then study its variation with age using observed and model color-magnitude sequences. The adopted  $g - i$  limits are listed in Table 5, and an example of this procedure (for M5) is shown in the top left panel in Figure 1.

We determine the *shape* of the photometric parallax relation by *simultaneously* fitting data for all five clusters. To do so, we first shift their  $r$  vs.  $(g - i)$  sequences to a uniform (arbitrary) magnitude scale by requiring that the median  $r$  magnitude for stars with  $0.5 < g - i < 0.7$  is 0. These offsets depend on the cluster metallicity, as discussed below. We then fit a parabola to all the data points, as a function of the  $g - i$  color, using unweighted least squares method (a third order polynomial is unnecessary to within

$\sim 0.05$  mag). We used the  $g - i$  color because it has better signal-to-noise properties than  $g - r$  and  $r - i$  colors. We did not use the so-called “projection on stellar locus” technique developed in Paper I because it produces essentially identical results for relatively bright stars considered here. The stellar locus parametrization from Paper I can be used to express the fiducial sequence in terms of the  $g - r$  and  $r - i$  colors, if needed.

The best-fit fiducial sequence is

$$M_r^0(g - i) = -2.85 + 6.29(g - i) - 2.30(g - i)^2, \quad (1)$$

with  $M_r^0 = r - \langle r \rangle = M_r - \langle M_r \rangle$ , valid for  $0.3 < (g - i) \lesssim 1.0$ , and the medians evaluated in the  $0.5 < g - i < 0.7$  color range. As discernible from the cluster data shown in the top right panel in Figure 1, individual clusters follow the mean relation to within 0.1 mag or better (the rms scatter for all data points around the best-fit relation is 0.08 mag). We compare the slopes of the predicted and observed sequences using the difference in absolute magnitudes at  $g - i = 0.4$  and at  $g - i = 0.7$  (the predicted value is 1.25 mag). The largest discrepancies of  $\sim 0.1$  mag are observed for M13 (the observed sequence is steeper) and M15 (the observed sequence is shallower). These discrepancies may be caused by a combination of metallicity and age effects.

We proceed by *assuming* that the *shape* of color-magnitude sequence given by eq. 1 is a universal function independent of metallicity, and that its *normalization* depends only on metallicity. While this is not strictly true, as we discuss below, the available data are not sufficient to robustly constrain the shape variation as a function of metallicity (and possibly other parameters, e.g. helium content, see Demarque & McClure 1980).

We place the color-magnitude sequences for each cluster on an absolute scale using distances from Harris (1996). The offset of the measured globular cluster sequences relative to the best-fit fiducial sequence is a strong function of metallicity. We improve observational constraints on this relation by considering six additional clusters discussed by Vandenberg & Clem (2003). We used their figures to estimate for each cluster its  $M_V$  at  $B - V = 0.60$  (corresponding to  $g - i = 0.57$ ), listed in Table 6. The corresponding  $M_r$  (i.e. the  $V - r$  color) are computed using the SDSS to Johnson system transformations from Ivezić et al. (2007).

The data shown in the bottom left panel in Figure 1 strongly suggest a non-linear relationship (without the extended metallicity baseline thanks to the Vandenberg & Clem data, the five SDSS clusters would imply a linear relationship). The best-fit parabola is

$$\Delta M_r([Fe/H]) = 4.50 - 1.11 [Fe/H] - 0.18 [Fe/H]^2, \quad (2)$$

where  $\Delta M_r$  is defined by

$$M_r(g - i, [Fe/H]) = M_r^0(g - i) + \Delta M_r([Fe/H]). \quad (3)$$

The rms scatter around the best-fit relation is 0.05 mag for the eleven clusters used in the fit, with the maximum deviation of 0.08 mag. This remarkably small scatter around a smooth best-fit function suggests that the determination of  $\Delta M_r([Fe/H])$  offsets for individual clusters has a similar precision. Note, however, that the overall scale of  $M_r(g - i, [Fe/H])$  includes all systematic errors inherent in cluster distances that are adopted from Harris (1996) compilation (including a possible covariance with cluster metallicity). The adopted relation produces gradients of  $dM_r/d[Fe/H] = -0.57$  mag/dex at the median halo metallicity ( $[Fe/H] = -1.50$ ), and  $-1.0$  mag/dex at the median thin disk metallicity ( $[Fe/H] = -0.2$ ), with an offset of 1.05 mag between these two  $[Fe/H]$  values.

The distributions of differences between the  $r$  band magnitudes predicted using the above expressions and the observed values for individual stars are consistent with expected noise due to photometric errors for all five clusters (see the bottom right panel in Figure 1 for an example based on M5). At the faint end ( $r \sim 21$ ), the expected uncertainty in  $M_r$  is about 0.3 mag (random error per star), and is dominated by random photometric errors in the  $g - i$  color. At the bright end, the  $g - i$  errors ( $\sim 0.03$  mag) contribute an  $M_r$  uncertainty of  $\sim 0.15$  mag, and an error in  $[Fe/H]$  of 0.1 dex results in  $M_r$  error of  $\lesssim 0.1$  mag. The random errors in the  $g - i$  color and photometric metallicity are by and large uncorrelated because the  $u$  band errors dominate the latter.

The SDSS cluster data discussed here are not sufficient to extend the fiducial sequence beyond  $g - i \sim 1$ . While not required for the analysis presented here, we extend for completeness the adopted relation using the *shape* of the “bright” relation from Paper I. Expressed as a function of the  $g - i$  color,

$$M_r^0(g - i) = -1.93 + 4.39(g - i) - 1.73(g - i)^2 + 0.452(g - i)^3, \quad (4)$$

valid for  $(g - i) > 0.8$ . We test this extension further below.

## C.2 Testing

Using SDSS observations for five clusters listed in Table 5, we first determined median photometric metallicity for each cluster, using best-fit expressions derived in this work. To avoid contamination by disk stars and noisy metallicity estimates, we only use stars with  $0.3 < g - i < 0.5$  and  $u < 21.5$ . Remarkably, the photometric metallicity estimates are consistent with the values taken from Harris (1996) to within  $\sim 0.1$  dex. This test ensures that eq. 2 can also be used with photometric metallicity estimates.

We have tested eqs. 1-3 using an independent sample of clusters observed by SDSS at distances beyond our cutoff of 12 kpc (NGC 4147, NGC 5053, NGC 5466, NGC 5024 and Pal 5). The first four clusters have low metallicities ( $[Fe/H] \sim -2.0$ ), and for Pal 5  $[Fe/H] = -1.41$ . The  $r$  vs  $g - i$  ridge lines predicted by eq. 1 agree well with the observed sequences (the data are much more noisy than for the first five nearer clusters due to fainter apparent magnitudes). The only significant discrepancy is observed for Pal 5, for which the predicted magnitudes are too faint by  $\sim 0.5$  mag (using a distance of 23.2 kpc).

To test the extension of photometric parallax relation to red colors, we use the  $M_V(B - V)$  sequence for M dwarfs with the Hipparcos data, as compiled in Fig. 17 from VandenBerg & Clem (2003): for  $B - V = (1.2, 1.3, 1.4)$ , corresponding to  $g - i = (1.51, 1.70, 1.93)$ , we adopt  $M_V = (7.5, 8.0, 8.5)$ . Assuming that metallicity of those stars is equal to the median thin disk metallicity,  $[Fe/H] = -0.13$  (Nordström et al. 2004; Allende Prieto et al. 2004), we obtain  $M_V = (7.42, 7.91, 8.54)$ . For the reddest data point with  $V - I = 2.0$ ,  $M_V = 9.5$ , and we obtain  $M_V = 9.47$ . This good agreement suggests that the extension given by eq. 4 is accurate to within  $\sim 0.1$  mag for  $g - i < 2.2$ .

For redder colors ( $g - i > 2.0$ ), we compared our results with the relation derived by Bochanski et al. (2008, in prep.), which is based on ground-based trigonometric parallaxes for nearby stars (Golimowski et al. 2008, in prep.). Assuming a median metallicity of  $[Fe/H] = -0.13$  for these stars, we found that the performance of eq. 4 starts deteriorating around  $g - i = 3.0$ . In the range ( $2.0 < g - i < 2.8$ ), our relation agrees with the Bochanski et al. relation within 0.07 mag (rms) and  $\sim 0.03$  mag (median), and maximum deviation  $< 0.1$  mag, evaluated on a grid with 0.01 mag step. A linear relation in the range  $2.8 < g - i < 4.0$

$$M_r^0(g - i) = -4.40 + 3.97(g - i) \quad (5)$$

is a much better approximation to the observed sequence than eq. 4 (but for a detailed fit please consult Bochanski et al.). Note that for  $[Fe/H] = -0.13$ , this relation must be shifted by 4.64 mag to get  $M_r$  (c.f. eq. 2).

As an additional test of the relation derived here, we compare it to color-magnitude sequences measured by Clem, VandenBerg & Stetson (2008) for three clusters that have turn-off color bluer than  $g - i = 0.6$  (M3, M13 and M92). Their data were obtained in the SDSS “prime” system, and we used expressions from Tucker et al. (2006) to transform those sequences into the SDSS survey system. For  $g - i > 0.5$ , their sequences for M3 and M13 are in good agreement ( $< 0.2$  mag) with our predictions, while for blue colors close to the turn-off color, they become progressively brighter as expected (see the top left panel in Figure 2). For M92, discrepancies are larger than  $\sim 0.2$  mag even for red colors ( $g - i \sim 1$ ). However, based on photometric transformations from Tucker et al. (2006)

and Ivezić et al. (2007), we find that the M92 sequence in the SDSS “prime” system from Clem, VandenBerg & Stetson (2008) and the M92 sequence in Johnson system from VandenBerg & Clem (2003) are not consistent. For example,  $V = 20.9$  at  $B - V = 0.6$  taken from VandenBerg & Clem implies  $r = 20.7$ , while data listed in Table 3 from Clem, VandenBerg & Stetson imply  $r = 20.45$  at the corresponding color. We emphasize that the same photometric transformations result in good agreement for the other two clusters, and that color-magnitude sequence for M92 from VandenBerg & Clem agrees with our relation to within 0.1 mag.

The top left panel in Figure 2 shows a comparison of the relation derived here with the three sequences from Beers et al. (2000). Similarly to the comparison with the Clem, VandenBerg & Stetson sequences, our relation predicts fainter magnitudes for blue turn-off stars, as expected. We emphasize that these differences are not due to errors in color-magnitude sequences adopted by Beers et al. because they agree with other sources, e.g. with VandenBerg & Clem (2003) data. Rather, the differences are due to our design choice to exclude from fitting the parts of the clusters’ color-magnitude sequences that are too close to their turn-off color.

Our results show that the Beers et al. spline interpolation of metallicity effects based on only three clusters performs remarkably well. The largest overall discrepancy between our photometric parallax relation and the three Beers et al. sequences for red colors ( $g - i > 0.6$ ) is observed for 47 Tuc: for  $1.0 < g - i < 1.8$ , the predicted  $M_r$  are too bright by 0.4 mag. Since agreement at our fiducial  $g - i \sim 0.6$  is satisfactory, this difference implies that the color-magnitude sequence for 47 Tuc is steeper than for other clusters discussed here. This peculiarity of 47 Tuc has been known for some time and may be related to its anomalous helium content (Demarque & McClure 1980; Hesser, Harris & Vandenberg 1987). We note that our relation predicts absolute magnitudes for red stars ( $B - V > 1$ ) that are brighter by  $\sim 0.3$  mag than the data for extremely metal-rich ( $[Fe/H] = +0.37$ ) open cluster NGC 6791 from VandenBerg & Clem (2003).

### C.3 Age effects and Comparison with Models

By design, the photometric parallax relation derived here avoids the increased curvature of the color-magnitude sequence close to the turn-off color. Its blue edge is constrained by the parts of M3 and M15 sequences that are *redwards* from their turn-off colors (see Table 5 and the top right panel in Figure 1). For stars with turn-off colors, the predicted absolute magnitudes can be up to  $\sim 1$  mag too faint. For example, for M5 turn-off stars selected by  $0.25 < g - i < 0.35$  ( $\langle r \rangle = 18.6$ ), the difference between predicted and observed  $r$  band magnitudes is well described by a gaussian distribution with a mean of 0.22 mag

and  $\sigma = 0.49$  mag, implying underestimated distances by 11% on average.

The effect of age on turn-off color and absolute magnitude, as a function of metallicity, can be gauged with the aid of model isochrones, e.g., such as those developed for SDSS photometric system by Girardi et al. (2004). While modeling difficulties prevent absolute normalization of such models to better than  $\sim 0.1$ - $0.2$  mag even for hot stars (and much worse for stars with  $g - i > 1$ ), their *relative* behavior, as a function of age, provides a valuable guidance. Girardi et al. models show that the turn-off color is bluer than  $g - i = 0.6$  even for 13 Gyr old populations and the metallicity at the upper end of the range relevant here ( $[Fe/H] = -0.4$ ). Hence, the adopted relation is insensitive to age effects for  $g - i > 0.6$ . For  $g - i < 0.6$ , it needs to be corrected as a function of metallicity and age.

The mean ages of halo and disk stars considered in this work can be estimated from the blue edge of their color distributions. The number of stars drops precipitously bluer than  $g - i \sim 0.25$  for low-metallicity subsample ( $Fe/H \lesssim -1$ , halo stars), and at  $g - i \sim 0.4$  for higher-metallicity subsample (disk stars). Interestingly, the Girardi et al. models suggest similar age for both subsamples:  $\sim 10$  Gyr, with an estimated uncertainty of  $\sim 2$  Gyr (due to metallicity and color zeropoint uncertainties; we adopted 0.2 dex and 0.05 mag, respectively). Motivated by this result, we derive an age correction appropriate for stars with median halo metallicity and age of  $\sim 10$  Gyr using the color-magnitude sequence for cluster M13 ( $[Fe/H] = -1.54$ ). For  $0.22 < g - i < 0.58$

$$\Delta M_r^{M13}(g - i) = -2.17 + 6.64(g - i) - 5.00(g - i)^2, \quad (6)$$

which increases from 0 at the red edge to  $-0.95$  mag at  $g - i = 0.22$ , and has to be added to the right-hand side of eq. 3.

This correction for age is not strictly applicable to stars with higher disk-like metallicity. However, the Girardi et al. models suggest that the error is small,  $< 0.2$  mag for  $g - i > 0.45$  (i.e. 0.05 redder than the turn-off color for disk stars), as illustrated in the top right panel in Figure 2. For this reason, we adopt eq. 6 as a universal age correction for stars bluer than  $g - i < 0.58$ .

Given different expressions for three color ranges (eqs. 1, 4, and 5) and the above age correction, for convenience we fit a fifth-order polynomial to a vector of  $M_r$  values generated using the appropriate expressions for  $0.2 < g - i < 4.0$  with a step size of 0.01 mag. Our *final* expression

$$M_r^0(g - i) = -5.06 + 14.32x - 12.97x^2 + 6.127x^3 - 1.267x^4 + 0.0967x^5, \quad (7)$$

where  $x = (g - i)$ , reproduces individual  $M_r$  values with an rms of 0.05 mag and maximum deviation below 0.1 mag. Together with eqs. 2 and 3, this is the final photometric parallax relation used in this work.

We have compared a large number of Girardi et al. models that span the relevant range of metallicities ( $-2.3 < [Fe/H] < 0$ ) and ages (1–13 Gyr) with the resulting photometric parallax relation. Model predictions are in good agreement (an rms of  $\sim 0.1$  mag) with the  $M_r$  vs.  $[Fe/H]$  dependence described by eq. 1, but model  $M_r$  are systematically too faint by  $\sim 0.2$  mag (evaluated at  $g - i = 0.7$ ). Possible explanations for this difference are i) model stars are too small by  $\sim 10\%$ , ii) model  $g - i$  color is too red by 0.06 mag, and iii) model  $[Fe/H]$  scale is offset relative to SDSS scale by  $\sim 0.3$  dex to larger values. A plausible combination of these effects, e.g. an error of 3% in sizes, 0.02 mag in color and 0.1 dex in metallicity, brings data and models into agreement (the probability that all three effects would have the same sign is 12%).

#### C.4 Comparison with SDSS Distances and J08

With the adopted age correction (eq. 6), our final expression is expected to produce very similar distances to those published in SDSS Data Release catalogs for blue stars ( $g - i < 2$ ). We have confirmed that this is the case: the median offset of implied  $M_r$  evaluated in small bins of  $u - g$  and  $g - r$  color (see the bottom left panel in Figure 2) is  $-0.07$  mag, with an rms of 0.06 mag. These differences are smaller than the intrinsic errors of the photometric parallax method ( $\sim 0.1$ - $0.2$  mag).

Using eqs. 2, 3, and 7, we can now determine “effective” metallicity that the two photometric parallax relations proposed in Paper I correspond to, as a function of the  $g - i$  color (see the bottom right panel in Figure 2). As designed, those two relations bracket the median halo metallicity ( $[Fe/H] = -1.50$ ) at the blue end, and sample the thin/thick disk metallicity range at the red end.

In summary, the relations proposed here are in good agreement ( $< 0.1$  mag) with clusters M3 and M13 at the low-metallicity end for  $g - i < 1.5$ , and with local stars with trigonometric parallaxes for  $g - i > 1.5$ . At a fiducial color  $g - i = 0.6$ , in the middle of the color range where photometric metallicity can be estimated, the rms scatter around the best-fit  $\Delta M_r$  vs.  $[Fe/H]$  curve is 0.08 mag. Even in cases of known peculiar behavior (e.g. 47 Tuc) and at the high metallicity end (e.g. NGC 6791), discrepancies do not exceed 0.4 mag. Compared to the Beers et al. relations utilized by SDSS, here we provide an estimate of the scatter around mean relations, a closed-form expression for the metallicity dependence, and extend the method’s applicability further into red to  $g - i \sim 4$ . Given the larger number of globular clusters observed in SDSS system utilized here, as well as tests based on external data sets, it is likely that distance estimates for main sequence stars based on photometric parallax method (both using relations derived here and the Beers et al. relations) do not suffer from systematic errors larger than  $\sim 10\%$ . While these

systematic distance errors are not overwhelming, they may have an impact on analysis of the Milky Way kinematics. We further discuss such issues in Paper III.

## REFERENCES

- Allende Prieto, C., Barklem, P.S., Lambert, D.L. & Cunha, K. 2004, *A&A*, 420, 183
- Beers, T.C., et al. 2000, *AJ*, 119, 2866
- Clem, J.L., VandenBerg, D.A. & Stetson, P. 2008,
- Demarque, P. & McClure, R.D. 1980, *ApJ*, 242, 5
- Girardi, L., Grebel, E.K., Odenkirchen, M. & Chiosi, C. 2004, *A&A*, 422, 205
- Harris, W.E. 1996, *AJ*, 112, 1487
- Hesser, J.E., Harris, W.E., Vandenberg, D.A., et al. 1987, *PASP*, 99, 739
- Nordström, B., Mayor, M., Andersen, J., et al. 2004, *A&A*, 418, 989
- Simones, J., Newberg, H.J. & Cole, N. 2008, *BAAS* (AAS Meeting #211)
- Tucker, D.L., Kent, S., Richmond, M.W., et al. 2006, *AN*, 327, 821
- VandenBerg, D.A. & Clem, J.L. 2003, *AJ*, 126, 778

Table 5. The Globular Clusters Observed by SDSS and Used in Photometric Parallax Analysis

Name	D <sup>a</sup>	R <sup>b</sup>	[Fe/H] <sub>H</sub> <sup>c</sup>	[Fe/H] <sub>ph</sub> <sup>d</sup>	N <sup>e</sup>	g <sup>i</sup> <sub>min</sub> <sup>f</sup>	g <sup>i</sup> <sub>max</sub> <sup>g</sup>	Δr <sup>h</sup>
M 2	11.5	10.0	-1.62	-1.66	472	0.40	0.70	0.00
M 3	10.4	17.5	-1.57	-1.41	1279	0.35	0.80	0.03
M 5	7.5	17.5	-1.27	-1.27	1776	0.40	1.10	-0.07
M 13	7.7	15.0	-1.54	-1.65	829	0.40	1.00	0.06
M 15	10.3	12.5	-2.26	-2.09	676	0.30	0.70	0.01

<sup>a</sup>Distance, in kpc, taken from Harris (1996).

<sup>b</sup>Angular radius (arcmin) used for selecting cluster stars, taken from Simones, Newberg & Cole (2008)

<sup>c</sup>Metallicity, taken from Harris (1996)

<sup>d</sup>Median photometric metallicity for stars with  $0.3 < g-i < 0.5$  and  $u < 21.5$

<sup>e</sup>The number of stars used for estimating  $[Fe/H]_{ph}$  (errors are dominated by systematics)

<sup>f</sup>The minimum  $g-i$  color used in analysis (determined by turn-off stars)

<sup>g</sup>The maximum  $g-i$  color used in analysis (determined from  $r < 21.5$ )

<sup>h</sup>The median  $r$  band offset (mag) for stars with  $0.5 < g-i < 0.7$ , relative to a prediction based on eqs. 1–3 (using distances listed in the second column).

Table 6. Additional Cluster Data from VandenBerg & Clem (2003)

Name	$[Fe/H]^a$	$M_V^b$	$M_V^c$
M 92	−2.50	6.30	6.32
M 68	−2.01	6.25	6.18
47 Tuc	−0.71	5.35	5.37
Pleiades	−0.11	4.80	4.79
M 67	−0.04	4.75	4.72
Hyades	+0.12	4.50	4.53

<sup>a</sup>Metallicity, taken from VandenBerg & Clem (2003), except for 47 Tuc, which is taken from Beers et al. (2000) (VandenBerg & Clem adopted −0.83, which produces 0.1 mag fainter  $M_V$  prediction).

<sup>b</sup>The absolute  $V$  band magnitude for  $B - V = 0.60$ , determined with an accuracy of 0.05-0.10 mag from figures presented in VandenBerg & Clem (2003).

<sup>c</sup>The absolute  $V$  band magnitude for  $B - V = 0.60$  determined using eqs. 1–3, and SDSS to Johnson transformations from Ivezić et al. (2007).

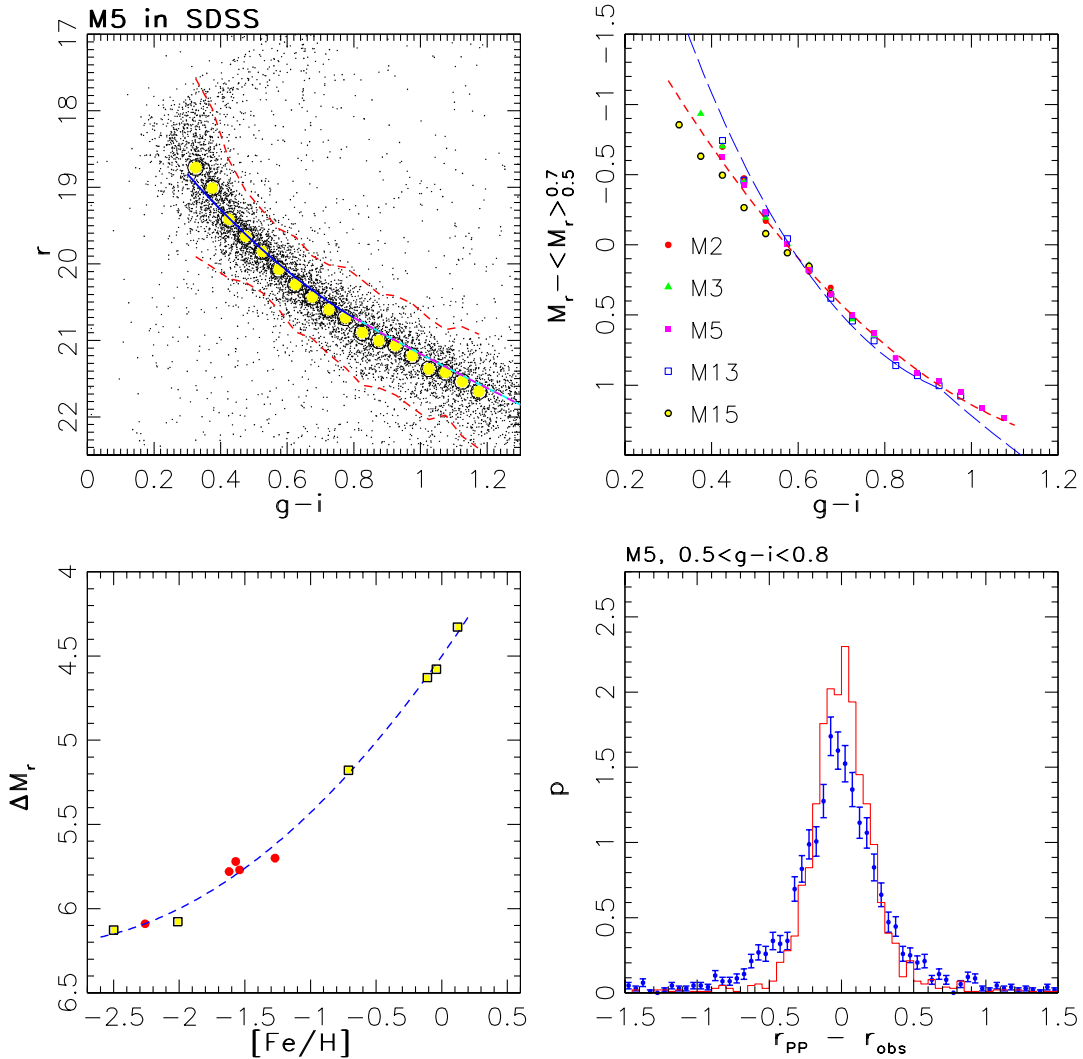


Fig. 1.— The top left panel shows the color-magnitude diagram for globular cluster M5 measured by SDSS. Individual stars are displayed as small dots, and the large dots show binned medians. The two dashed lines show the  $2\sigma$  envelope around these medians, and the solid line is the prediction based on adopted photometric parallax relation (see text). The top right panel shows analogous binned medians for five globular clusters, with each sequence rescaled by the median magnitude for stars with  $0.5 < g - i < 0.7$ . The short-dashed line shows a best-fit fiducial sequence (eq. 1). For a comparison, the long-dashed line shows the  $[Fe/H] = -2.20$  fiducial sequence from Beers et al. (2000). The dots in the bottom left panel show the absolute magnitude offsets relative to the fiducial relation for five globular clusters listed in Table 5. The squares show analogous offsets for six globular cluster listed in Table 6. The dashed line is the best unweighted linear fit to both data sets (eq. 2). The symbols with error bars (representing counting noise) in the bottom right panel show the distribution of differences between  $r$  band magnitudes predicted using the adopted photometric parallax relation and the observed values. The histogram shows the expected scatter due to photometric errors.

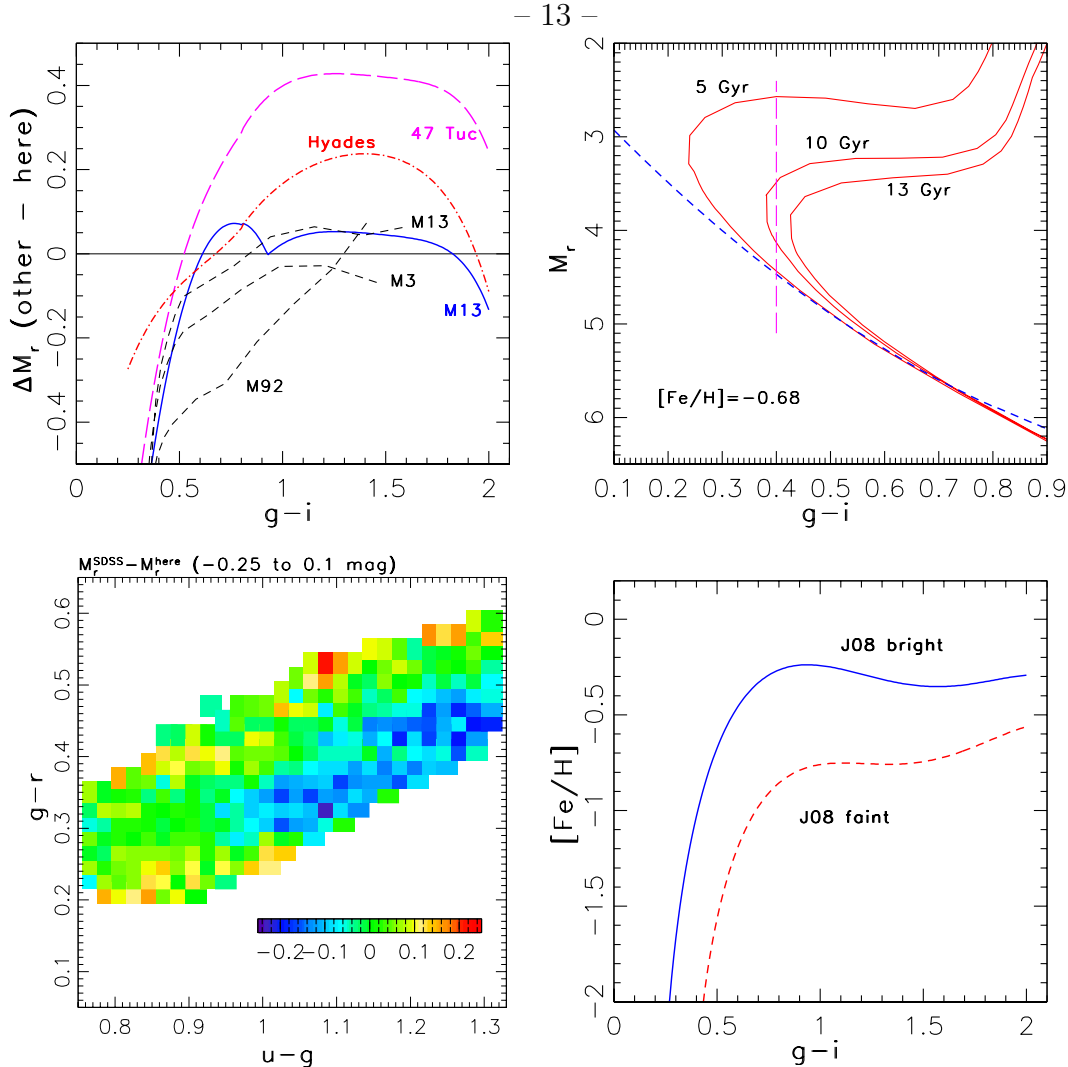


Fig. 2.— The top left panel shows the difference between the color-magnitude sequences from Beers et al. (2000) for three metallicity values (solid:  $-2.20$ ; long-dashed:  $-0.71$ ; dot-dashed:  $+0.12$ ), and eqs. 1-3 derived here. The three short-dashed lines shows analogous differences for M3, M13 and M92 sequences from Clem, VandenBerg & Stetson (2008), as marked. The systematic differences for blue stars are due to age effects. The solid lines in the top right panel show  $M_r$  for a Girardi et al. (2004) model with  $[Fe/H] = -0.68$ , evaluated for three ages, as marked. The models are offset by 0.2 mag to brighter magnitudes. The short-dashed line shows  $M_r$  computed using eqs. 1 and 7. The vertical long-dashed line marks the turn-off color for disk stars. The bottom left panel shows the median differences between the SDSS distance modulus for main-sequence stars (determined using the Beers et al. sequences) and the values estimated using eq. 7, color-coded as shown in the inset. The two methods agree at the  $\sim 0.1$  mag level. The bottom right panel shows implied metallicity, estimated using eqs. 1 and 7, for the two photometric parallax relations proposed by Jurić et al. (2008; solid line: “bright” relation; dashed line: “faint” relation). At the blue end, they bracket the median halo metallicity ( $[Fe/H] = -1.50$ ), and at the red end they sample the thin/thick disk metallicity range.